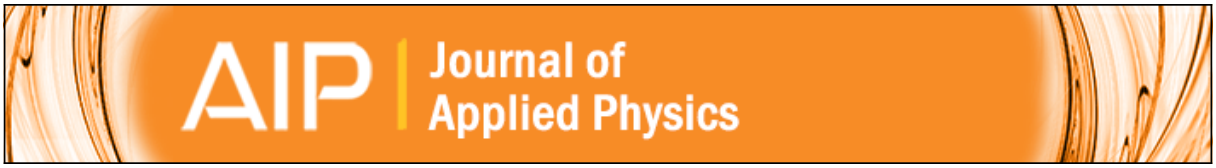

Magnetic force images of nanomagnetic domains taken with platinum-coated tips

O. Teschke, M. U. Kleinke, M. E. R. Dotto, D. M. Soares, M. Knobel, and E. F. de Souza

Citation: Journal of Applied Physics **94**, 626 (2003); doi: 10.1063/1.1579546

View online: http://dx.doi.org/10.1063/1.1579546

View Table of Contents: http://scitation.aip.org/content/aip/journal/jap/94/1?ver=pdfcov

Published by the AIP Publishing

Magnetic force images of nanomagnetic domains taken with platinum-coated tips

O. Teschke,[a] M. U. Kleinke, M. E. R. Dotto, D. M. Soares, and M. Knobel
NanoStructures and Interfaces Laboratory, Instituto de Fisica–UNICAMP, 13083-970 Campinas, SP, Brazil

E. F. de Souza
Instituto de Ciencias Biologicas e Quimica, Pontificia Universidade Catolica de Campinas, 13020-904 Campinas, SP, Brazil

(Received 12 December 2002; accepted 11 April 2003)

This article deals with magnetic force microscope images of nanosized domains in Co-coated films made by Pt-coated tips as well as micromagnetic images of data tracks written in recording media. Pt-coated tips have improved image delineation of the magnetic field distribution compared to images obtained by Co-coated hard magnetic tips. The force acting on Pt-coated tips in the magnetic field of the substrate was modeled assuming a paramagnetic tip. Due to the ferromagnetic nature of the interaction between the tip and substrate the spatial resolution of hard magnetic tips was shown to be inadequate to measure details of the features of nanosized domains. A comparison of the magnetic images made by Pt-coated tips with topographic images shows that magnetic domains resist thermal erasure at ambient temperature when they are formed of eight metallic grains. [DOI: 10.1063/1.1579546]

I. INTRODUCTION

Magnetic force microscopy (MFM) is a well-established method used to probe the micromagnetic structure of samples.[1–5] However, it generally only allows an approximate pattern of the stray field distribution above a sample. The reason is that the magnetization distribution, stray field, coercivity and effective volume of the magnetic tip effect on the imaging are not known. Thin-film probes can be magnetized so as to sense particular field components, thereby simplifying image interpretation of samples.[6,7] Tips are most commonly magnetized along their axis, although lateral magnetizing fields can also be used.[8,9]

Many of the past improvements in the disk-drive capacity resulted from advances in the disk platter storage information density. The problem, though, is that, as one shrinks the size of the grains of the magnetic material to make smaller bits, the grains can lose their ability to hold a magnetic moment at a given temperature. It really comes down to the thermal stability of the media. Ultimately, the properties of the material media must be considered, such as the coercivity or magnetic stability, and how a few grains can be used to obtain the desired resistance to thermal erasure. However, the spatial resolution of magnetic force microscope hard magnetic tips is probably not adequate to measure the profile of such a structure.

This article describes magnetic field distributions that were imaged by both Pt-coated and hard magnetic Co-coated tips. Initially data tracks written in recording media were used to characterize the performance of the tips. Images taken using Pt-coated and Co-coated tips were compared in order to determine the effect of the magnetic properties of the tip on the image resolution. The magnetic substrate and the Pt-coated tip interaction were modeled. The nanosize magnetic domain structure of Co-coated films deposited on silicon and the grain size structure were imaged and the number of grains that form stable magnetic domains was determined.

II. EXPERIMENT

To image with magnetically hard MFM tips, we used a commercial ThermoMicroscopes Auto Probe CP scanning probe microscope (SPM), which measures magnetic force gradients by detecting shifts in phase or resonance frequency[10] of the oscillating cantilever probes. The cantilever was vibrated at the resonance frequency f_0 with 30 nm root-mean-square (rms) amplitude and was scanned with the tip 100 nm above the surface, about twice the designed flying height of the head above the disk. To image with Pt-coated MFM tips we used a TopoMetrix TMX2000 scanning probe microscope. All of the imaging shown here was recorded at room temperature. MFM cantilevers were microfabricated silicon diving boards with integrated tips.[10] The manufacturer coated the etched silicon pyramidal tips used in this work with platinum or cobalt. Co-coated and Pt-coated cantilevers with spring constants $\kappa_{sp}=1-5$ N/m, resonant frequencies $f_0=150$ kHz, and quality factors $Q\sim 270$ in air were used. Force versus separation curves were measured using a TopoMetrix TMX2000 atomic force microscope (AFM). Each curve was registered using at least three different tips with various approach velocities, and the average was evaluated using measurements at different points on the sample. Films of Co were deposited by magnetron sputtering from a Co target of 99.95% purity onto Czochralski-grown (100) Si substrates covered with a thin native oxide layer, using an ATC-2000 sputtering system from AJA International. The substrates were ultrasonically cleaned with a neu-

[a]Electronic mail: oteschke@ifi.unicamp.br

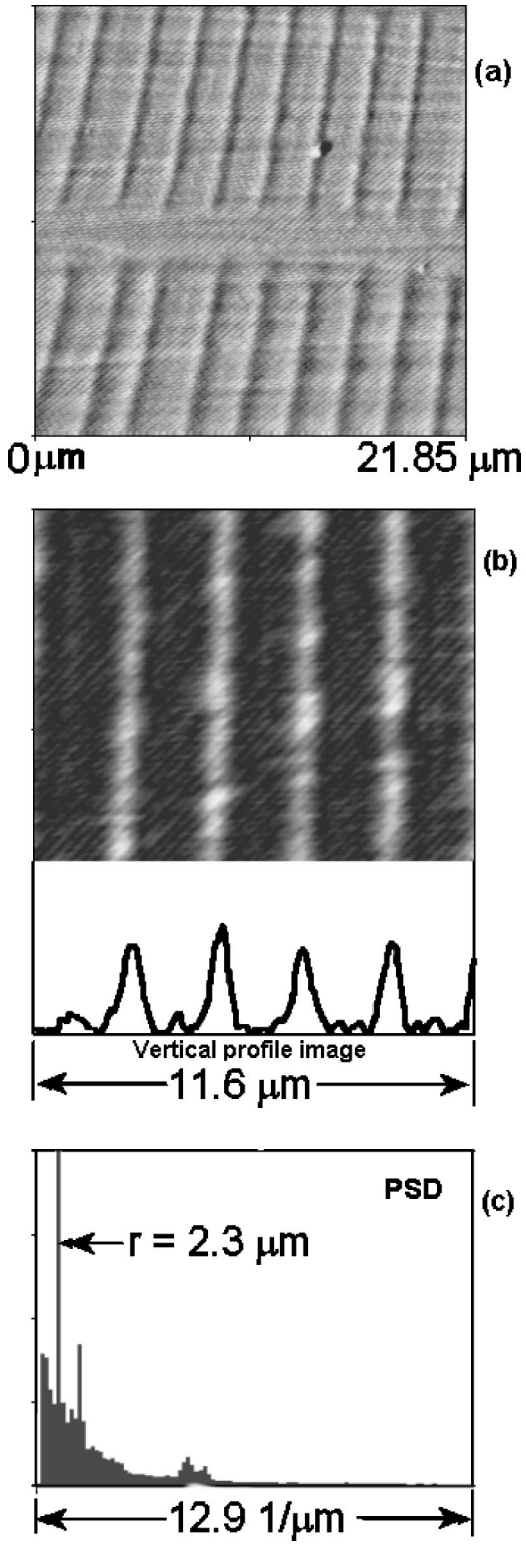

FIG. 1. (a) MFM data collected using a Pt-coated tip from a region of a hard disk in which ~2.3 μm transitions were written. (b) Vertical profile image (VPI) indicated by the horizontal continuous line and (c) the corresponding power spectrum density (PSD).

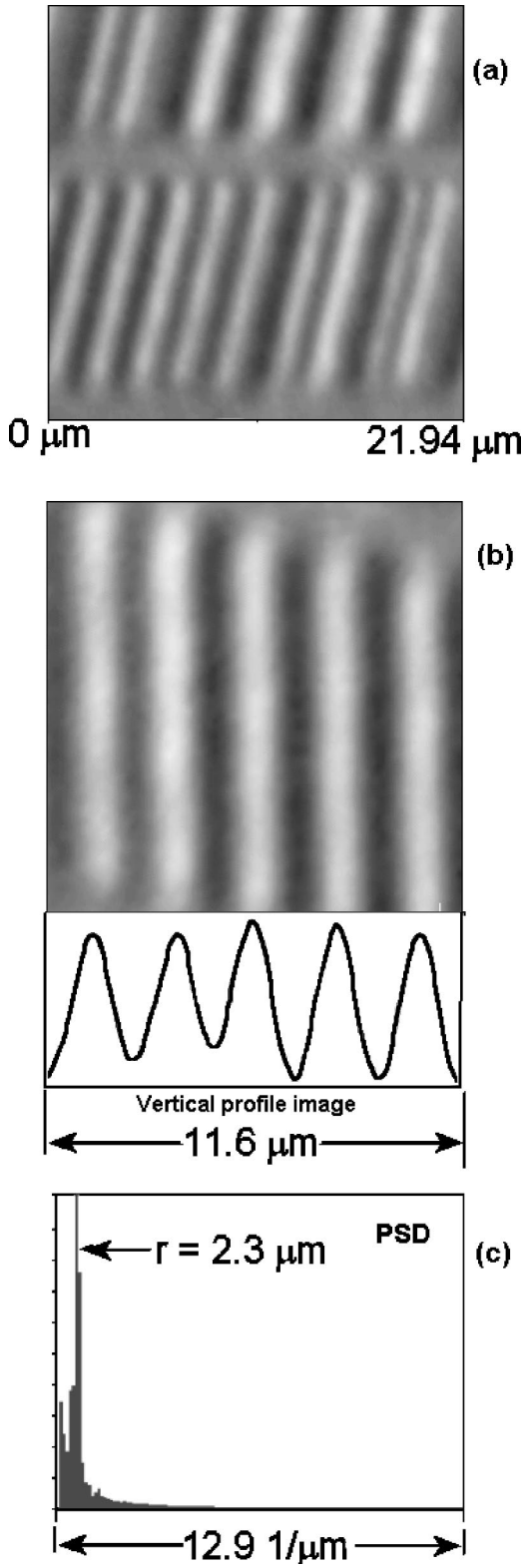

FIG. 2. (a) MFM data collected using a Co-coated tip from a region of a hard disk in which ~2.3 μm transitions were written. (b) Vertical profile image and (c) the corresponding power spectrum density.

tral detergent in de-ionized water for 30 min, then washed repeatedly with de-ionized water and ethyl alcohol. Finally, the substrates were dried in ultradry nitrogen. The films were kept at room temperature during deposition with an argon pressure of 5 mTorr. The thicknesses of the Co films were measured by Rutherford backscattering spectroscopy (RBS) and both scanning electron microscopy (SEM) and transmission electron microscopy (TEM). In the present work, three different samples were used: pure Co thin films with ~100 nm thickness, granular samples of $Co–Si–O_2$, also 100 nm

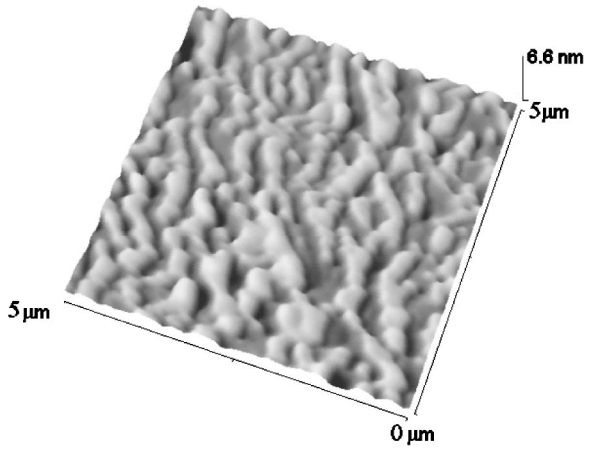

FIG. 3. MFM image from an area of a Co77 (77 vol % Co concentration) film sputtered on a Si substrate collected with a Pt-coated tip.

thick, where the Co concentration is 77 vol % (Co77) and granular samples of Co whose concentrations are 51 vol % (Co51). For the Co77 case the concentration is above the percolation threshold, and therefore the film behaves similarly to pure Co films.

A cylindrical shaped permanent magnet with a 2 cm diameter, length of 1 cm and measured $|\overline{B}|$ value of $\approx$0.1 T was used to modify the film's magnetic domain structure. The permanent magnet was deposited on the top of the Co-coated silicon substrate.

III. RESULTS

To establish the nature of the platinum tip response low-density transition recording media were examined. Figure 1(a) shows data from the MFM image collected from one area of a sample in which transitions were written at $\sim$2.3 μm spacing [Fig. 1(c)]. The tips were all scanned along the direction of the written data track. The images show two profiles simultaneously, with scratches observed at $\sim$10° off angle to the scanning direction and a sequence of bits that form the written track observed at $\sim$90° off angle. The scratches characterize the topography of the hard disk surface. Figure 1(b) shows the vertical profile image (VPI) of the parallel stripes while Fig. 1(c) shows the power spectrum density (PSD).

To investigate the origin of the interaction that generated the images obtained with the Pt tips, let us now compare this image with the one with Co-coated tips from the same hard disk sample. The result is shown in Fig. 2. Figure 2(a) shows a pattern of lines that form the written track of the hard disk and displays the sequence of bits. Figure 2(b) shows the VPI of the parallel stripes and Fig. 2(c) the PSD. The same sequence of parallel lines with distinct separation is shown in both Figs. 1 and 2. Then the sequence of bits displayed in the image obtained by scanning the hard disk surface with Pt-coated tips [Figs. 1(a) and 1(b)] shows that the contrast registered is magnetic in origin.

It is also clear both visually [Figs. 1(a) and 2(a)] and from the VPI that the platinum tip allows the written signals to be more readily resolved than the Co-coated tip does. The VPI and PSD show that the Co-coated tip image predominantly depicts the fundamental frequency, while the platinum tip VPI shows higher spatial frequency components. Similar results have been found with a number of platinum tips.

Co77 films on Si substrates were then examined. Figure 3 shows a MFM image obtained with Pt-coated tips collected from an area of a sample in which one can distinguish magnetically ordered regions that vary from $\sim$250 to $\sim$35 nm. Figure 4 shows an image from the same area of the sample scanned with a Co-coated tip. The measured width of the magnetic domains is almost uniform and equal to $\sim$560 nm; consequently the presence of tip magnetization causes an increase in the image dimensions of the magnetic features.

In order to determine the grain size of the coated film, images were collected with Si_3N_4 tips in contact mode (AFM) which show the grain morphology. The result is depicted in Fig. 5.

To unambiguously demonstrate the magnetic origin of the contrast in the images obtained with Pt-coated tips, regions of thin Co-coated films were scanned. The result is shown in Fig. 6. Then, this image was compared to the new image from approximately the same region (space shift of $\sim$10 μm) after interaction of the film with a permanent mag-

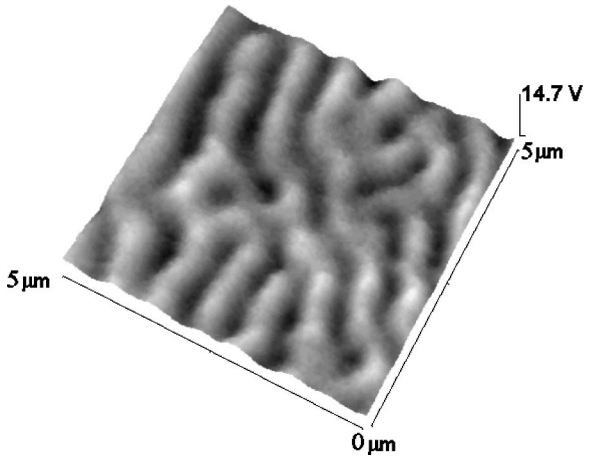

FIG. 4. MFM image of the same area as that shown in Fig. 3 collected with a Co-coated tip.

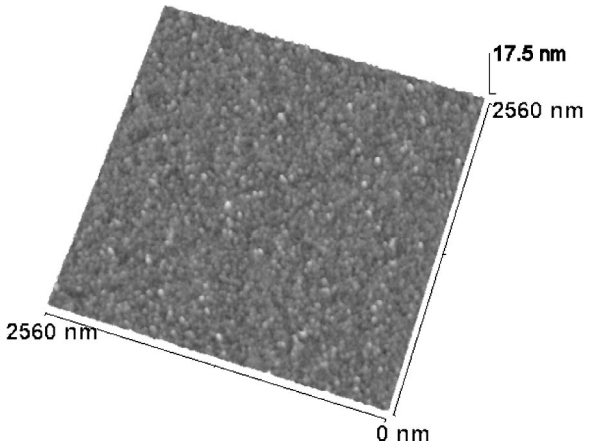

FIG. 5. AFM image of the same area as that shown in Fig. 3 collected with a Si_3N_4 tip showing the grain morphology.

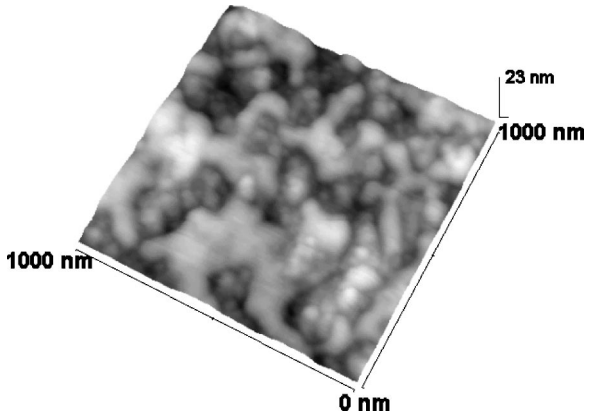

FIG. 6. MFM image of an area of Co77 (77 vol % Co concentration) film sputtered on a Si substrate collected with a Pt-coated tip.

net. The result is shown in Fig. 7. The size of the magnetically oriented regions increased substantially.

The approaching force curve on a substrate is a plot of the change in cantilever deflection (δy) versus sample displacement (δx). On a hard nondeformable surface, y is proportional to x while the tip and the sample are in contact. Rather than using the sample position (x), it is more useful to use an absolute distance (H) that is relative to the separation between the tip and the sample surface. The correction to produce a force–distance curve uses the relationship $H = \delta x - \delta y$.[11,12] The following force curves show the force versus absolute distance plots.

Force versus separation curves were measured for Pt-coated tips using nonmagnetic substrates, i.e., polished silicon surfaces. Figure 8 shows the force versus separation curves for Pt-coated tips in air for a Si substrate (open circle) and for a Co51 film on a Si substrate (closed circle). Various force versus separation curves were measured after scanning the substrate and choosing points at the registered images that correspond to the maximum value of $|\overline{B}|$ on the surface and the maximum amplitude was registered. The averages of five maximum amplitude force values are displayed on each curve. The distinct features of this curve compared to the ones measured for Si substrates are attraction of the tip at

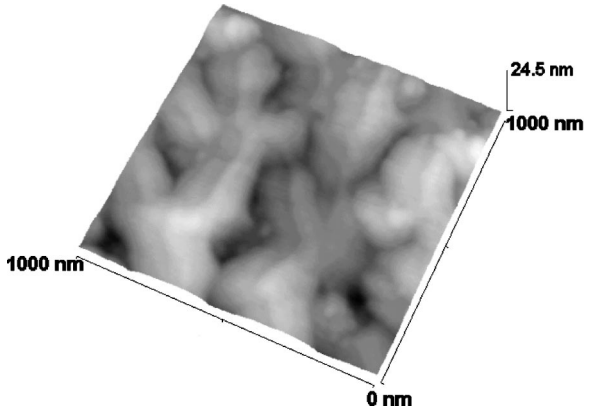

FIG. 7. MFM image of approximately the same area as that shown in Fig. 6 (space shift of <10 μm), after interaction of the film with a permanent magnet ($B \approx 0.1$ T).

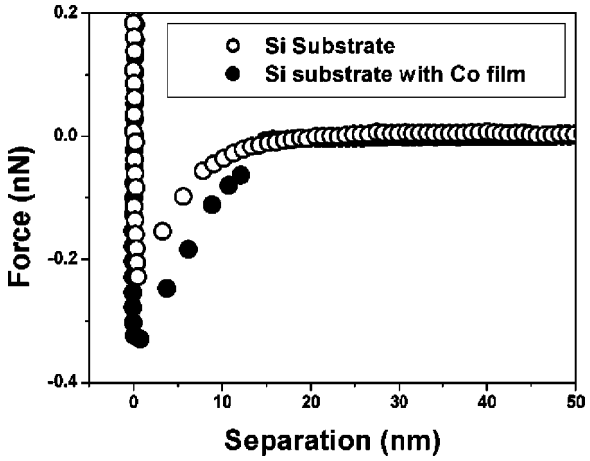

FIG. 8. Force vs separation curve measured using a Pt-coated tip for a Si substrate (open circle) and for a Co51 film on a Si substrate (closed circle).

distances far from the interface compared to the attraction observed for Pt-coated tips and Si substrates and a force amplitude increase by a factor of 2. Figure 9 shows a force versus separation curve at the maximum intensity field locations measured for a hard disk substrate, using Co-coated tips previously magnetized. Observe that the magnetic force contribution increased from approximately 0.2 to 10 nN, an increase of approximately a factor of 50. The magnetic field range extended ~90 nm from the substrate.

IV. DISCUSSION

A stray magnetic field emanating from the surface of a sample generates force on a magnetic tip, which is attached to a flexible cantilever. A sensitive deflection sensor is used to detect cantilever motion and hence the force (or force gradient). To form an image, the strength of the sample–tip interaction is mapped as a function of the position on the sample. In order to show that the contrast is magnetic in origin, sequences of bits that form the written track of hard disks were imaged by both Co-coated and Pt-coated tips.

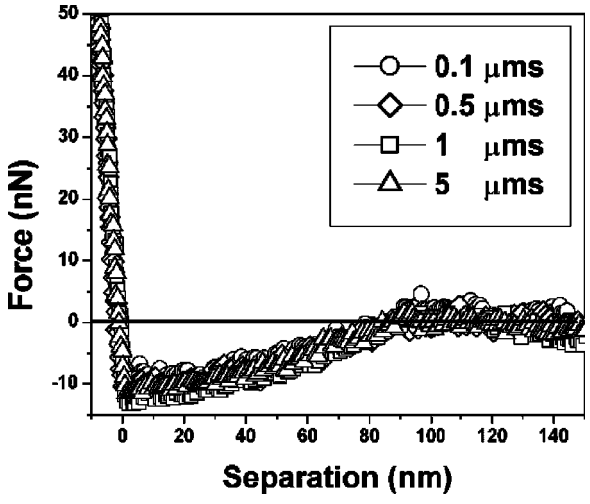

FIG. 9. Force vs separation curve measured using a Co-coated tip for a Co51 film on a silicon substrate (○: $v = 0.1$ μm/s, ◇: $v = 0.5$ μm/s, □: $v = 1$ μm/s and △: $v = 5$ μm/s.

Figure 1(a) shows the sequence of bits imaged by Pt-coated tips and Fig. 2(a) that imaged by Co-coated tips. It is clear that the pattern measured is associated with the written track in both configurations since the distance between the bits is not periodic, consequently images are not the result of an oscillatory regime of the cantilever. The second feature observed is that the thicknesses of the imaged bits are distinctive.

Further verification of the magnetic origin of the contrast in the registered images is shown by a comparison of Figs. 6 and 7. Initially an area of the film was scanned and the image shows domains that have width of ~200 nm. The head of the microscope was then removed and a permanent magnet ($B \approx 0.1$ T) was brought into contact with the Co films. After a few minutes the permanent magnet was removed and approximately the same area previously imaged was scanned by the cantilever tip. The result is shown in Fig. 7. A comparison of the images shows that the magnetic field of the permanent magnet has altered the size of the magnetic domains.

The minimum force that can be detected is determined by the sensitivity of the deflection sensor which is typically around 0.01 nm. With a 1 N/m cantilever, this deflection corresponds to a minimum detectable force of $F_{\min} \approx 0.01$ nN. If in Fig. 8 we subtract the contribution associated to capillarity and electric forces (open circle) from the magnetic force (closed circle), we obtain at the Co film/air interface $\Delta F \approx 0.2$ nN. This force is 20 times larger than the minimum detectable force previously estimated.

The tip/substrate interaction present during immersion of the Co-coated tip in the substrate film magnetic field was previously described;[13–17] the Pt-coated tip/substrate interaction is going to be discussed next. The tip was defined as having a sharpened conical shape with one flat end with area of πr^2. The magnetic density $\vec{B}(z)$ is determined by the normal component of the magnetization vector of the ferromagnetic film.

A. Model of tip–surface interaction

The expression derived for the diamagnetic interaction is given in the Appendix. The calculated values of the force acting on the tip for $B(D \approx 0) \approx 0.055$ T is shown in Fig. 11 by the dashed line and its maximum value at the film surface is $\sim 10^{-14}$ N. This force is three orders of magnitude smaller than the minimum detectable force previously estimated as 0.01 nN.

We then assume a paramagnetic interaction between the tip and substrate. In order to verify this hypothesis we calculated the MFM force acting on the tip during its immersion in the magnetic field of the film for Pt-coated tips with a magnetic susceptibility of $\chi = 4\pi \times 21 \times 10^{-6}$.[18] A schematic diagram of tip immersion in the region is depicted in Fig. 10. The elemental volume (dv) of the trapezoidal tip immersed in the substrate magnetic field is given by $dv = \pi(R + z \tan \alpha)^2 dz$ and the change in magnetic energy in immersion of the tip with a magnetic susceptibility χ in the stray field of the substrate is calculated by integrating the energy over the tip immersed volume in the magnetic field. Recently

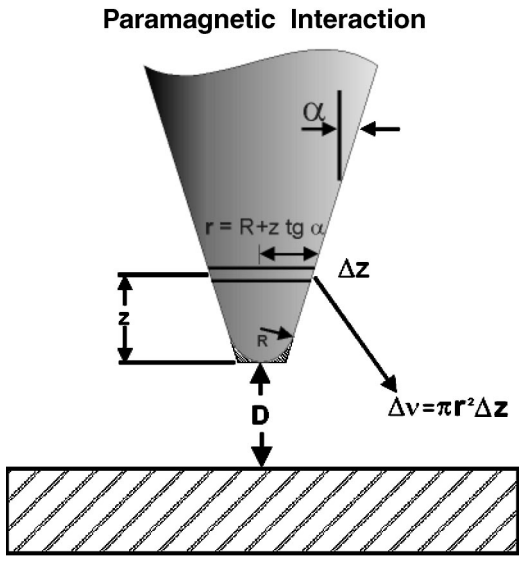

FIG. 10. Schematic diagram of the tip and magnetic substrate paramagnetic interaction associated with the exchange of a region on the top of the magnetic substrate with magnetic permeability μ_0 by a Pt-coated tip with magnetic permeability $\chi = 4\pi \times 21 \times 10^{-6}$.

a similar expression was derived for electric interaction between the tip and substrate.[19] The force is obtained by the gradient of the energy expression, i.e., $F_z = (-\partial \Delta W)/\partial z$, where

$$\Delta W = \int \frac{B_z^2(z)}{\mu_0} \pi (R + z \tan \alpha)^2 \left(1 - \frac{1}{1+\chi}\right) dz. \qquad (1)$$

To compare the experiments with calculations, we fit the force versus separation curves to the gradient in Eq. (1). The best results of fitting the force versus separation curve measured for Co77 films is shown in Fig. 11 by the dotted line. The maximum calculated value for force F acting on the tip for $|\overline{B}(D=0)| \approx 0.055$ T and $R = \sim 25$ nm is 0.1 nN, and this value is four orders of magnitude larger than the calculated diamagnetic force so a paramagnetic tip/substrate tip is very likely to be responsible for the imaging effect. Figure 11 also

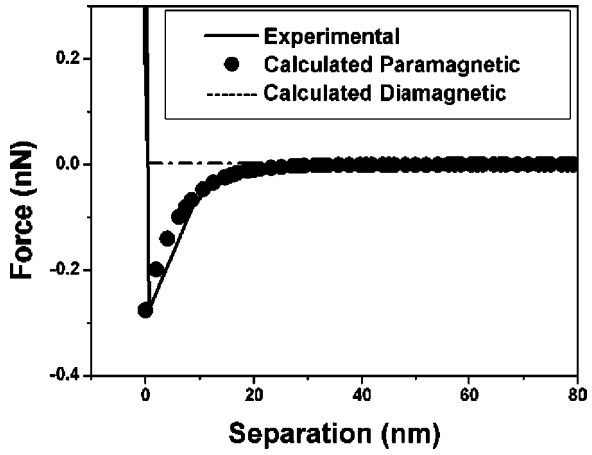

FIG. 11. Difference (solid line) between the magnetic force curves in Fig. 8 measured using a $Co_x(SiO_2)_{1-x}$ magnetic substrate (open circle) and a nonmagnetic substrate (closed circle). Force calculated (closed circle) using Eq. (2) for $B(D=0) = 0.055$ T, tip radius 250 nm and $\chi = 4\pi \times 21 \times 10^{-6}$; diamagnetic force (dash-dotted line).

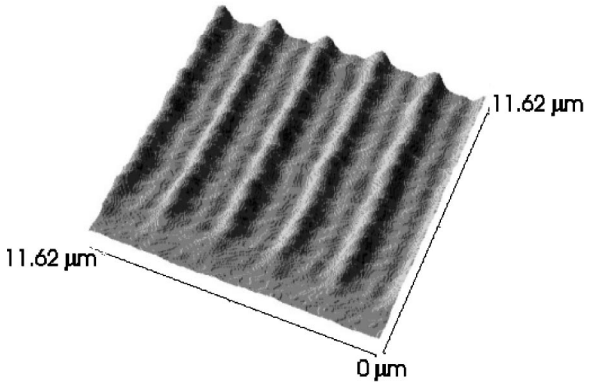

FIG. 12. Reconstructed image of data shown in Fig. 1(b) collected by a Pt-coated tip, which corresponds only to the harmonics of the fundamental spatial frequency indicated in the PSD.

shows that the model fits the measured curves for reasonable values of the magnetic field $B \approx 0.055$ T at the film interface.

A MFM operating with Pt-coated tips images simultaneously magnetic and topography features, as shown in Fig. 1(a). Separating the magnetic and topographic influences on the cantilever's behavior could be a difficult task in some samples. However the results displayed in Figs. 1 and 11 show that this is not the case in the observed configuration, indicating that the magnetic force at the scanned tip/substrate distance is larger than the forces involved in topographic imaging. This fact is confirmed when we compare the force acting on the tip as it approaches a nonmagnetic substrate (open circle in Fig. 8) and a magnetic film (closed circle in Fig. 8).

The three-dimensional image shown in Fig. 12 was obtained from the one shown in Fig. 1(a) by selecting only the harmonics of the fundamental spatial period $(2.3\ \mu\text{m})^{-1}$ shown in Fig. 1(c) by the PSD. For comparison, a three-dimensional (3D) image of the sample scanned with the Co-coated tip is shown in Fig. 13. It is possible to observe that, using the Co-coated hard magnetic tip, the highest data track density is the one displayed by the hard disk; but using Pt-coated tips, it is possible to obtain a density reading at least two times higher. Consequently, the presence of tip magnetization causes broadening in the image as seen in the comparison of Figs. 3 and 4 and Figs. 12 and 13.

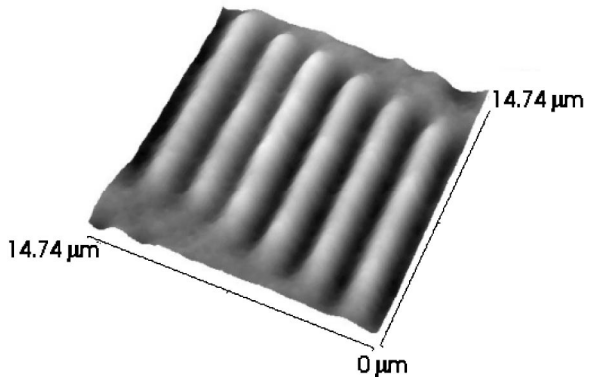

FIG. 13. Reconstructed image of data shown in Fig. 2(b) collected by a Co-coated tip displayed for comparison.

B. Magnetically correlated nanograins

Let us now address another part of our work associated with the increase in the information density stored in disk platters. As one shrinks the size of the grains in magnetic material, the grains can come close to the point of holding a magnetic moment at a given temperature. The analysis in Fig. 4 compared to the one shown in Fig. 3 indicates that scanned images with hard magnetic tips do not have adequate resolution to measure such a structure; only Pt-coated tip scanned images display regions, which we call ''magnetic clusters,'' that can be considered small magnetic domains; inside this the orientation of each particle moment is highly correlated to that of neighbors.[20] By comparing Figs. 3 and 5 it is possible to determine how few morphological grains form magnetic clusters that could show the desired thermal stability at ambient temperature. This was accomplished by measuring the area of the individual magnetic domains in Fig. 3 and the average area of individual morphological grains shown in Fig. 5 (obtained using Si_3N_4 tips) modeled as single objects in the image analysis program.[21] By counting the number of single objects and clusters and measuring the area of each single object it is possible to determine the average of how many morphological grains (Fig. 5) form a magnetic cluster (Fig. 3). The result is that small, isolated magnetic domains are formed by an average of eight morphological grains of Co sputtered grains. These isolated eight grain particles have remanence and coercivity, resulting in images with 35 nm diameters when scanned with Pt-coated tips. This result is in full agreement with recent results obtained for $Co-Si-O_2$ granular samples, where the nanostructure was indirectly inferred from magnetic data.[20] In that work, Denardin *et al.* explained their results within the framework of independent 3D magnetic clusters that involve around 25 particles. In fact, it corresponds to the observation of the formation of a collective magnetic state arising from dipolar and exchange interactions among individual particles (also called ''superferromagnetic'' by some authors[20]).

Unlike Co and other ferromagnetic tip coatings, magnetic properties of the individual particles in films should not be altered by the tip when scanning with Pt-coated tips. A study of the erasure resistance of the domains of Co sputtered samples as a function of the temperature is then possible using images scanned by Pt-coated tips. The state of the art magnetic recording bit size is $4\ \mu\text{m} \times 0.2\ \mu\text{m}$ with a transition width of ~ 20 nm.[22] The results shown in this work indicated that platinum tips conform images of the magnetic structure of the magnetic domains as well as of the transition region.

V. CONCLUSIONS

Images made with Pt-coated tips display magnetic features. The spatial resolution of hard magnetic tips was shown to be inadequate to measure nanosized domain features. The magnetic substrate interaction with Pt-coated tips was modeled and shown to be associated with the paramagnetic nature of the Pt-coated tips. The magnetic nanosized domains

in Co77 films were shown to be formed by about eight morphological grains when imaged using Pt-coated tips.

ACKNOWLEDGMENTS

The authors are grateful to Professor F. Missell (IF/USP, São Paulo, Brazil) for kindly providing Co films and to J. R. Castro and L. O. Bonugli for technical assistance and acknowledge economical support from CNPq Grant No. 523.268/95-5 and FAPESP Grant No. 98/14769-2.

APPENDIX

The diamagnetic interaction is given by Faraday's law. The current induced by immersion of the Pt-coated tip into the substrate magnetic field results in an induced tip magnetic moment which has opposite orientation relative to that of the substrate's magnetic field direction. In the analysis of the platinum tip response we treat the cantilever tip as a medium with resistivity ρ and the tip approaches the sample surface along the axis perpendicular to the sample plane. A schematic diagram of tip immersion in the region is depicted in Fig. 10, where z is the integration variable of trapezoidal volume and D is the distance between the surface and the end of the tip. Since the cantilever vibrates at resonance frequency ω_0 we assume that the current induced on the tip has the same frequency dependence. If the emf induced in the elemental ring is given by Faraday's law $\int \vec{E}\cdot\vec{dl}=\int \dot{B}\cdot\vec{ds}$, i.e., $E_\phi=(\dot{B}_z r)/2$ where $\vec{E}$ is the electric field, then the elemental magnetic moment is written as $\Delta M(z,D)=\pi(R+z\tan\alpha)^3[\dot{B}_z(z,D)]/(3\rho)$. The magnetic energy involved in immersion of the tip in the $\vec{B}$ region is given by $\Delta W=\frac{1}{2}\int d\overline{M}\cdot\overline{B}(z)$. Force is obtained by the gradient of the energy expression, i.e., $F_z=(-\partial\Delta W)/\partial z$, where

$$\Delta W=\int \pi\omega_0 B_z^2(z)\,\frac{(R+z\tan\alpha)^3}{3\rho}\,dz. \tag{A1}$$

We tried to fit the force versus separation curves with the gradient of the above equation and the results are shown in Fig. 11 by the dashed line.

[1] Y. Martin and H. K. Wickramasinghe, Appl. Phys. Lett. **50**, 1455 (1987).
[2] A. Moser, H. J. Hug, I. Parashikov, B. Stiefel, O. Fritz, H. Thomas, A. Baratoff, H. J. Guntherodt, and P. Chaudhari, Phys. Rev. Lett. **74**, 1847 (1995).
[3] P. Grutter, A. Wadas, E. Meyer, H. Heinzelmann, H. R. Hidber, and H. J. Guntherodt, J. Vac. Sci. Technol. A **8**, 406 (1990).
[4] H. J. Mamin, D. Rugar, J. E. Stern, R. E. Fontant, and P. Kasiraj, Appl. Phys. Lett. **55**, 318 (1989).
[5] T. Ohkubo, Y. Maeda, and Y. Koshimoto, IEICE Trans. Electron. **E78-C**, 1523 (1995).
[6] D. Rugar, H. J. Mamin, P. Guethner, S. E. Lambert, J. E. Stern, I. McFadyen, and Y. Yogi, J. Appl. Phys. **68**, 1169 (1990).
[7] K. Babcock, M. Dugas, S. Manalis, and V. Elings, Mater. Res. Soc. Symp. Proc. **355**, 311 (1995).
[8] P. Grutter *et al.*, Appl. Phys. Lett. **57**, 1820 (1990).
[9] K. Babcock, M. Dugas, V. Elings, and S. Loper, IEEE Trans. Magn. **30**, 4503 (1994).
[10] Park Scientific Instruments, User's Guide to Autoprobe CP, Part II, California (1998).
[11] O. Teschke, G. Ceotto, and E. F. de Souza, J. Vac. Sci. Technol. B **18**, 1144 (2000).
[12] O. Teschke, G. Ceotto, and E. F. de Souza, Chem. Phys. Lett. **326**, 328 (2000).
[13] J. Lohau, S. Kirsh, A. Carl, G. Dumpich, and E. F. Wassermann, J. Appl. Phys. **86**, 3410 (1999).
[14] J. Lohau, S. Kirsh, A. Carl, and E. F. Wassermann, Appl. Phys. Lett. **76**, 3094 (2000).
[15] T. R. Albrecht, P. Grutter, D. Horne, and D. Rugar, J. Appl. Phys. **69**, 668 (1991).
[16] R. Proksch, G. D. Skidmore, E. D. Dahlberg, S. Foss, J. J. Schmidt, C. Merton, B. Walsh, and M. Dugas, Appl. Phys. Lett. **69**, 2599 (1996).
[17] M. W. Coffey, J. Appl. Phys. **86**, 3917 (1999).
[18] R. Becker, *Electromagnetic Fields and Interactions* (Dover, New York, 1982), Vol. 1.
[19] O. Teschke and E. F. de Souza, Appl. Phys. Lett. **74**, 1755 (1999).
[20] J. C. Denardin, A. L. Brandl, M. Knobel, P. Panissod, A. B. Pakhomov, H. Liu, and X. X. Zhang, Phys. Rev. B **65**, 064422 (2002).
[21] IMAGE PRO-PLUS, Ver. 4.1 for Windows, Media Cybernetics.
[22] J. B. Kortright, D. D. Awschalom, J. Stohr, S. D. Bader, Y. U. Idzerda, S. S. P. Parkin, I. K. Schuller, and H. C. Siegmann, J. Magn. Magn. Mater. **207**, 7 (1999).